INDUCTIVELY COUPLED PLASMA FOR HIGHLY EFFICIENT AND LOW DAMAGE RESIST STRIPPING

Stephen Savas

Mattson Technology, Inc.
Fremont, CA 94538

ABSTRACT

A new plasma source using inductively coupled plasma (ICP) excitation has been developed that offers several advantages over more commonly used microwave-based sources, including low generation of damaging species such as charged particles and UV radiation and less heat production by the plasma. The new ICP source is inherently more efficient in producing the neutral reactive (atomic and molecular) oxygen species active in the strip process. A range of damage and contamination tests, including measurements of wafer charging, mobile metal and heavy metal contamination, and minority carrier lifetime degradation, confirm that the ICP source produces less wafer charge damage and contamination than typical microwave systems. This paper discusses the fundamental physics of the ICP source and presents results of computer modeling studies using a Boltzmann code which explain the overall increase in performance. The calculations give the distribution of electron energies in the plasma along with the rate constants for the high energy inelastic collision processes which produce oxygen dissociation, ionization, and UV excitation. These calculations show that in the ICP source, less than 0.3% of the power goes into the production of charged particles and UV radiation, and about 17% goes into the production of heat. The ICP source therefore requires less heavily baffled gas flow and generates a much lower heat load on the plasma chamber walls, making it much more compatible with advanced process chemistries such as those using fluorine.

Presented at the 1st International Symposium
on Plasma Process-Induced Damage, May 13-14, 1996
Santa Clara, California, U.S.A.

I. INTRODUCTION

Wafer contamination, specifically by mobile metals such as sodium, is believed to be highly dependent on the flux of charged particles and UV radiation at the wafer surface.[1] To reduce this flux in the wafer process chamber and achieve low sodium contamination levels, microwave-based strip systems have separate plasma and process chambers. The plasma chambers are made of quartz, sapphire or similar materials, and extensive baffling is required downstream in the gas flow to filter charged particles and UV radiation. This approach has significant disadvantages, including materials compatibility issues that limit the use of advanced strip processes, for instance those using fluorine chemistries, due to etching of chamber walls and quartz components.

Recently, Mattson Technology, Inc., began shipping its new generation resist strip system, which uses an inductively coupled plasma (ICP) source. Test data for this system show very low levels of wafer charge damage and contamination by both heavy metals and mobile ions. At the same time, excellent strip rates and uniformity characteristics have been achieved. The Mattson ICP strip system produces levels of contamination and wafer charge damage that are comparable to, or lower than, those of typical microwave-based systems. It achieves these results without the need for quartz baffles or right-angle bends in small diameter tubing. In this paper, we show that this performance is due in large part to the fundamental physics of the ICP plasma source, which reduces the production of ions and UV radiation and which is more efficient in producing neutral oxygen atoms by dissociation of oxygen molecules.

This paper describes computer modeling results which show that the ICP plasma is more efficient in dissociating oxygen molecules than typical microwave systems while also producing less heat. The computer modeling studies used the Boltzmann code ELENDIF obtained from the National Center for Atmospheric Research. First, the electron energy distribution for electrons in the oxygen plasma was calculated. The program then integrated the energy distribution with the cross sections for oxygen dissociation, ionization and excitation to determine the rate constants for generation of oxygen atoms, charged particles and UV radiation by electron impact processes in the plasma. The percentage of plasma power which goes into heating the oxygen atoms to become a heat load on the plasma chamber walls was also obtained. Calculated characteristics of the ICP source are compared with those of typical microwave-based sources of oxygen atoms, based on measurements reported in the literature.[2]

II. DAMAGE AND CONTAMINATION RESULTS

A number of different charge damage and contamination tests were performed to characterize the Mattson ICP strip system, including measurements of wafer charging, mobile metal contamination, heavy metal contamination, and minority carrier lifetime degradation. For these tests, the wafers were processed about 20 cm from the visible lower boundary of the ICP plasma. Results in field tests are found to be better than those of typical microwave-based systems in avoiding damage and contamination.

Extensive wafer charging studies were performed using floating electrode devices, including both "CHARM" wafers[3] and MNOS capacitors.[4] These studies showed no net electrical charging within experimental error of antenna structures in the direct and unbaffled downstream gas flowing from the plasma. The "CHARM" wafers, which contained floating gate EEPROM devices with varying degrees of sensitivity to UV and charge exposure, had sensitivities nominally on the order of 2 - 3 V. The MNOS capacitors, which retain the charge from the plasma exposure on the exposed electrode, with a resulting flatband voltage shift, had sensitivities on the order of 0.1 V or less.

Measurements of sodium drive-in contamination were performed using Quadrupole SIMS analysis at Charles Evans Associates. These measurements gave sodium concentrations from $3x10^9$ to $5x10^9$ atoms/cm^2 after exposure to the ICP process, including 100% overetch. The lower concentration value was the average obtained while using an ion/UV screen placed about 5 cm above the wafer, while the higher value was obtained with no screen between the plasma and the wafer. CV measurements were also performed, and results of both methods were consistent.

In addition, the following tests were also performed with an ion/UV screen interposed between the plasma and the wafer. TXRF measurements of heavy metal concentrations showed the levels of all measured elements (calcium, chromium, manganese, iron, nickel, copper, and zinc) to be equal to those of controls (with sensitivity $8x10^{10}$ atoms/cm^2 for Ca; $3x10^{10}$ for Cr; $1x10^{10}$ for Mn, Ni, and Cu; $10x10^{10}$ for Fe; and $100x10^{10}$ atoms/cm^2 for Zn). Measurements of minority carrier lifetime and diffusion length showed very clean films, with minority carrier lifetime $1.1x10^{-4}$ sec and diffusion length above 1000 μm. Measurements of the interface trap density and fixed charge density gave $7.2x10^{10}$ cm^{-2}, indicating very low levels of ionizing radiation from the plasma.

The following section discusses the fundamental physics of the ICP discharge and provides a foundation for the computer modeling results which follow.

Presented at the 1st International Symposium
on Plasma Process-Induced Damage, May 13-14, 1996
Santa Clara, California, U.S.A.

III. PHYSICS OF THE ICP DISCHARGE

In the Mattson ICP source, a high frequency (rf) electric current is passed through a helical coil which circles a dielectric-walled chamber to couple power into the electrons in the chamber. The Mattson ICP strip system is illustrated schematically in Figure 1. A multi-turn coil surrounds the cylindrical chamber, and the rf current in the coil creates a predominantly axial magnetic field within the chamber.

FIGURE 1. The Mattson ICP source and process chamber.

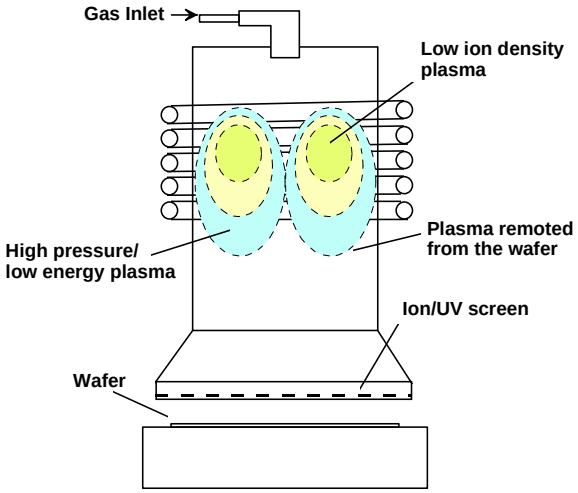

The magnetic field reverses direction at 13.56 MHz, the frequency of the rf generator, resulting in a very rapid periodic change in the magnetic flux parallel to the cylinder axis. This changing flux induces a circumferential electric field which is parallel to the walls of the cylinder. The equation which governs the induction electric field is given by

$$(2\pi r)\mathbf{E}_I = \frac{d}{dt}\int_S \mathbf{B}\cdot d\mathbf{A} \qquad (1)$$

where $\mathbf{E_I}$ is the induction electric field; **B** is the magnetic field vector; S is the circular surface over which the magnetic flux is integrated; r is its radius; and d**A** is a symmetric area element of the surface with a characteristic direction represented by the normal vector, perpendicular to the axis of the cylinder.

The peak magnitude of the induction electric field in the Mattson ICP source can be calculated using the measured currents in the induction coil. A maximum electric field strength of approximately 15 V/cm is obtained for operation at a pressure of 1 torr and a power level of 800 W, essentially our standard process conditions. This maximum field value applies to a volume adjacent to the chamber wall which is about a centimeter deep in the radial direction and which extends axially about 1.5 cm in both directions from the center turn. Figure 2 shows a contour map of the magnitude of the induction electric field, which decreases fairly quickly as the radius decreases, but more slowly as the axial position varies from the center of the coil. Visual inspection of the visible plasma shows it to be a thin toroid, consistent with the high field region (15 V/cm) found in this calculation. The volume occupied by the plasma is about 2.5 liters, much greater than that of typical microwave-based sources (20 - 50 cm^3).

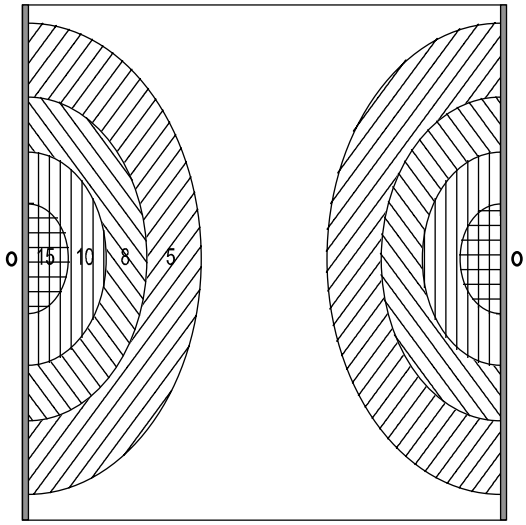

FIGURE 2. Contour map showing the magnitude of the peak induction electric field in the ICP source. The field varies radially inwards from a maximum of 15 V/cm to 5 V/cm and in both directions axially from the center turn of the induction coil.

The induction electric field sustains the plasma discharge as it drives electrons in a circumferential direction around the axis of the cylinder. Because the electric field has the same sinusoidal time dependence as the current in the coil, the electrons are driven alternately clockwise and counterclockwise at 13.56 MHz. As the electrons circulate, they make frequent collisions with gas molecules and atoms. Some of these collisions are elastic, so that electrons scatter without much energy loss. Some are inelastic, causing molecular excitations which result in dissociation, vibration, electron emission, or emission of radiation. Because the electrons scatter in random directions, they diffuse in the gas with nearly the same speed in all directions. (If they diffuse to regions with a lower electric field, their average energy and bulk velocity soon decrease.) The energy of random motion (thermal motion), approximately 2 eV, is much greater than the directed energy of bulk motion along the electric field for the conditions in the plasma. This energy of random motion is what goes into the inelastic collisions which produce the various neutral species and the ionization which sustains the plasma. The electron drift motion directed along the field produces the circulating electric currents within the plasma.

IV. COMPUTER MODELING RESULTS

Computer algorithms are available which employ the Boltzmann equation to calculate the electron energy distribution and the rate constants for electron impact processes with gas molecules for electrons driven in a time-independent electric field. The program used in our computer calculations was ELENDIF, written by Dr. Lowell Morgan and obtained from the National Center for Atmospheric Research. As input to the program we used cross sections[5] taken from the literature for the dominant inelastic collision processes of electrons with oxygen molecules and atoms as a function of the electron energy. The calculated results include the electron energy distribution (EED), given as a function of the induction electric field divided by the gas density, E/N.

As input to the ELENDIF program, we used E/N values representing a peak electric field ranging from 7 to 35 V/cm-torr. Values from about 5 to 15 V/cm-torr characterize our standard ICP process, as indicated earlier in Figure 2. Values near 35 V/cm-torr are characteristic of typical microwave-based sources, as discussed further below. Figure 3 shows the EED results for several values of the peak electric field. For higher values of E/N, the distribution of electron energies is shifted to higher values.

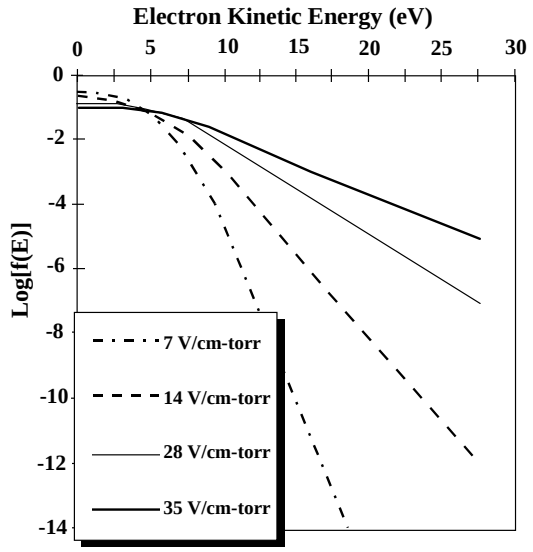

FIGURE 3. The electron energy distribution function calculated for different values of E/N, the induction electric field divided by the gas pressure (V/cm-torr).

The ELENDIF program integrates the resulting EED multiplied by the electron speed and the cross sections for inelastic collision processes. In this way, rate constants are calculated for processes which include ionization and molecular excitation followed by dissociation into atoms in the ground state and excited states. The calculated rate constants for dissociation, ionization, and UV excitation are summarized in the top half of Table I for several values of E/N. Since a time-independent electric field is assumed, the resulting electron energy distribution is an approximation to conditions in the plasma. This approximation causes the program to overestimate the rate constants (for a 13.56 MHz excitation at 1 torr) for high energy processes such as ionization, high energy dissociation (the 8.4 eV dissociation channel), and UV excitation relative to those for lower energy processes (such as the 6 eV dissociation channel and molecular excitation). This effect is discussed in more detail in the Appendix. As a result, the rate constants given in Table I for ionization and UV excitation are somewhat larger than the true values.

TABLE I. Calculation results for various values of E/N.

E/N:	**8 V/cm-torr**	**15 V/cm-torr**	**ICP average**	**30 - 40 V/cm-torr**
$k_{dissoc.}$	$1x10^{-10}$	$8x10^{-10}$	–	2 - $3x10^{-9}$
$k_{ioniz.}$	< $4x10^{-17}$	< $7x10^{-13}$	–	0.4 - $1.5x10^{-10}$
$k_{UV\ ex.}$	< $5x10^{-15}$	< $3x10^{-12}$	–	0.8 - $2x10^{-10}$
$k_{dissoc.}/k_{ioniz.}$	> $1x10^{6}$	> 1000	> 2000	20 - 50
$k_{dissoc.}/k_{UV\ ex.}$	$2x10^{4}$	> 200	> 500	15 - 25
Power ratio: ioniz./total	< $1x10^{-6}$	< $1x10^{-3}$	0.1%	0.7 - 2%
Power ratio: UV/total	< $1x10^{-4}$	< $5x10^{-3}$	0.2%	1.5 - 5%
Power ratio: heat/total	13%	22%	17%	35 - 46%
Heat/area	–	–	0.22 W/cm^2	1.5 - 5 W/cm^2
Ion current	–	–	10^{-5} A/cm^2	$>10^{-3}$ A/cm^2

Eliasson and Kogelschatz[5] have also performed the time-independent calculation to obtain the percentages of the electron energy which go into different oxygen excitation processes for a wide range of electric fields. Their results show that for the conditions (E/N values) pertaining to the Mattson ICP source, more than 80% of the power goes into oxygen excitation processes which produce less heat (including the $[a^1\Delta_g]$, $[b^1\Sigma_g^+]$, and $[A^3\Sigma_u^+]$ excitations and the 6 eV dissociation channel), while the amount of power going to produce ionization and UV excitation is very slight, < 0.3%. These results are summarized in the lower half of Table I. The fraction of power going into heat, including kinetic energy of the oxygen atoms (the Franck-Condon effect), is found to be about 17%. Thus, the Mattson ICP source at standard conditions of gas pressure, power density, and electric field is a very efficient producer of neutral species including excited oxygen atoms.

These results contrast with those of typical microwave-based sources of oxygen atoms used for resist stripping. Depending on the plasma source configuration, E/N values appropriate to microwave plasma sources fall in the range of 30 - 40 V/cm-torr, as determined from experimental data in Ref. 2. This range of values is reflected in the far right column of Table I. We used these values with the calculations of Eliasson and Kogelschatz[5] as above to determine the percentages of microwave power going into the various oxygen excitation, dissociation, and ionization processes for various source configurations. For these sources, the distribution of power is shifted towards higher energy dissociation (with its greater production of heat), ionization, and UV excitation, and away from the low energy oxygen excitation and dissociation which dominate in the ICP source. One indicator of this difference is the much greater visible brightness of the plasma region in microwave-based sources. The power fraction going into heat, including kinetic energy of the gas, varies from 35 to 46%, depending on the characteristics of the plasma source chamber.

The results summarized in Table I allow the following comparisons between the ICP source and typical microwave plasma sources:

(1) In the ICP source, the rate constant for dissociation is more than 2000 times the rate constant for ionization and more than 500 times that for UV excitation. In typical microwave systems, on the other hand, dissociation processes are much less dominant. Because of the larger volume of the plasma (50 - 100 times that of microwave systems), the ICP source has much higher production rates for the neutral excited oxygen species active in the strip process.

(2) The power flow to the walls in the ICP source is less than 0.25 W/cm^2; whereas the power flow to the walls in the microwave systems is between 1.5 - 5 W/cm^2.

(3) In the ICP source, about 0.3% of the input power goes to produce ionization and UV radiation; whereas in the microwave plasma source, between 2 - 7% of the input power goes into these processes, consistent with the much greater visible brightness of microwave plasmas.

(4) The ion current in the ICP source is on the order of 10^{-5} A/cm^2, while in typical microwave systems it is at least 100 times this amount.

(5) In the ICP plasma source, about 17% of the input power goes directly into heat; whereas for the microwave plasma source the percentage is from 35 to 46%, depending on the source configuration.

These results explain why more stringent charged particle and UV filtering is required for microwave plasma sources, which use physical constraints such as right-angle bends and baffles between the plasma and wafer. Moreover, in microwave plasma sources the greater heat and ion flux to the walls means higher etch rates of chamber walls and components. In the ICP source, on the other hand, the low heat and ion flux to the walls mean lower etch rates of the plasma chamber walls, thus permitting use of fluorinated chemistries.

IV. CONCLUSIONS

A new inductively coupled plasma (ICP) source has been developed for strip applications that produces no wafer charge damage and very low contamination by heavy metals and mobile metals such as sodium. A consideration of the fundamental physics of the new source show that it has superior efficiency in producing the neutral reactive oxygen species active in the strip process. More importantly, the ICP source has a lower production rate of damaging species such as charged particles and UV radiation, thus permitting less heavily baffled gas flow. Another characteristic is the greatly reduced heat and ion flux to the chamber walls. Consequently, the ICP source allows the use of many reactive gases with a much lower rate of wall erosion by sputtering or etching compared to microwave plasma sources. The ICP source therefore provides advanced strip capabilities with minimal impact on the plasma vessel lifetime.

V. APPENDIX

The program used for these calculations is accurate primarily in situations where the electric field is constant. When the electric field changes slowly relative to the energy loss time of an electron by inelastic collision, the reaction rate can be calculated by averaging the instantaneous reaction rate over an rf cycle. Since the inelastic collision rate is electron energy dependent, the accuracy of the electron energy distribution (EED) calculations, and therefore also the accuracy of the rate constant calculations, depends on the electron energy. Analysis shows that for high energy electrons (energy above about 9 eV), the rate constants for high energy electron collision processes are somewhat overestimated if the maximum field is assumed to be constant.

The origin of this overestimation can be understood from the following analysis of the electron collision rates, which depend on the scattering cross sections, which are functions of the electron energy. In the Mattson ICP source at standard conditions, the gas pressure is about 1 torr (about $2x10^{16}$ molecules/cm^3 at 150 ºC) and the thermal velocity of electrons is about 10^8 cm/sec. This means that low energy electrons (energy about 1 eV) make no more than about 10^7 inelastic collisions per second. Since this collision rate is less than the rf frequency (13.56 MHz, or $8.52x10^7$ rad/sec), the electron power loss rate is low during each rf cycle and the EED can be approximated by that for a time-independent electric field whose magnitude is given by the RMS average over the rf cycle (about 0.7 times the peak value of the electric field).

In contrast, for higher energy electrons (above about 9 eV), the inelastic collision frequency is several times 10^8 Hz, so that electrons undergo many high energy inelastic collision processes during an rf cycle and therefore have a higher energy loss rate. For these high energy electrons, the time-independent field approximation is therefore less accurate. In reality, the EED for high energy electrons modulates at the rf frequency as a function of the instantaneous electric field. The number of energetic electrons in this distribution varies exponentially with the instantaneous electric field, with a significant contribution to the high energy inelastic collision processes occurring only when the electric field is about 80% or more of its peak value. This time duration amounts to only about one third of the rf cycle. Since the high energy electrons also have higher power loss rates, the rate constants for the high energy inelastic processes are therefore overstated by the calculations discussed in the main body of this paper.

REFERENCES

1. Charles Boitnott, *Solid State Technol.*, Vol. 36 (1994), p 51.
2. Z. Zakrzewski *et al., Microwave Excited Plasmas*, Chapter 4, eds. Moisan and Pelletier (Elsevier, 1992).
3. W. Lukaszek *et al., Nucl. Instr. and Meth.* B55 (1991), p. 143; and *Proc. IEEE Int'l. Conf. on Microelectron. Test Structures*, Vol. 2, (1989). p 153.
4. Y. Kawamoto, *Extended Abstracts of the 17th Conf. on Solid State Dev. and Mat.*, (Japan Society of Applied Physics, Tokyo 1985), p 333; and K. Tsunokuni, K. Nojiri *et al., 19th Conf. on Solid State Dev. and Mat.*, (Japan Society of Applied Physics, Tokyo, 1987), p 195.
5. B. Eliasson and U. Kogelschatz, *Asea-Brown-Boveri Report KLR 86-11 C* (1986).